

Observation of Vanishing Charge Dispersion of a Nearly Open Superconducting Island

Bargerbos, Arno; Uilhoorn, Willemijn; Yang, Chung Kai; Krogstrup, Peter; Kouwenhoven, Leo P.; De Lange, Gijs; Van Heck, Bernard; Kou, Angela

DOI

[10.1103/PhysRevLett.124.246802](https://doi.org/10.1103/PhysRevLett.124.246802)

Publication date

2020

Document Version

Final published version

Published in

Physical Review Letters

Citation (APA)

Bargerbos, A., Uilhoorn, W., Yang, C. K., Krogstrup, P., Kouwenhoven, L. P., De Lange, G., Van Heck, B., & Kou, A. (2020). Observation of Vanishing Charge Dispersion of a Nearly Open Superconducting Island. *Physical Review Letters*, 124(24), [246802]. <https://doi.org/10.1103/PhysRevLett.124.246802>

Important note

To cite this publication, please use the final published version (if applicable).
Please check the document version above.

Copyright

Other than for strictly personal use, it is not permitted to download, forward or distribute the text or part of it, without the consent of the author(s) and/or copyright holder(s), unless the work is under an open content license such as Creative Commons.

Takedown policy

Please contact us and provide details if you believe this document breaches copyrights.
We will remove access to the work immediately and investigate your claim.

Observation of Vanishing Charge Dispersion of a Nearly Open Superconducting Island

Arno Bargerbos^{1,*}, Willemijn Uilhoorn¹, Chung-Kai Yang,² Peter Krogstrup,³ Leo P. Kouwenhoven,^{1,2} Gijs de Lange,² Bernard van Heck,² and Angela Kou²

¹*QuTech and Kavli Institute of Nanoscience, Delft University of Technology, 2600 GA Delft, The Netherlands*

²*Microsoft Quantum Lab Delft, 2600 GA Delft, The Netherlands*

³*Microsoft Quantum Materials Lab and Center for Quantum Devices, Niels Bohr Institute, University of Copenhagen, Kanalvej 7, 2800 Kongens Lyngby, Denmark*



(Received 22 November 2019; accepted 15 May 2020; published 19 June 2020)

Isolation from the environment determines the extent to which charge is confined on an island, which manifests as Coulomb oscillations, such as charge dispersion. We investigate the charge dispersion of a nanowire transmon hosting a quantum dot in the junction. We observe rapid suppression of the charge dispersion with increasing junction transparency, consistent with the predicted scaling law, which incorporates two branches of the Josephson potential. We find improved qubit coherence times at the point of highest suppression, suggesting novel approaches for building charge-insensitive qubits.

DOI: [10.1103/PhysRevLett.124.246802](https://doi.org/10.1103/PhysRevLett.124.246802)

The manipulation of single charge carriers has been one of the most important advances in condensed matter physics, enabling a wide range of nanoelectronic technology in areas such as detection, thermometry, and metrology [1–5]. The control of single charge carriers is made possible by the quantization of charge on mesoscopic islands well isolated from the environment. Charge quantization manifests as Coulomb oscillations: periodic dependence of the system's observables reflecting the energy cost of adding an additional charge to the system. As the coupling strength to the environment increases, quantum fluctuations progressively delocalize the charge, suppressing Coulomb oscillations. In normal state conductors, it is well known that this suppression occurs through single-electron tunneling [6–14].

In the case of superconducting islands, the coupling to the environment instead occurs via coherent Cooper pair tunneling. In conventional tunnel junctions, the latter is mediated by a large number of weakly transmitting transport channels, characterized by the Josephson energy E_J . In this case, the size of the charge dispersion depends only on the ratio between the charging energy E_c and E_J , as illustrated by the Cooper pair box ($E_J/E_c \approx 1$) [15] and the transmon ($E_J/E_c \gg 1$) [16]. The Cooper pair box has large charge dispersion, whereas for the transmon charge, dispersion is exponentially suppressed in the ratio E_J/E_c [16,17]. This behavior originates from quantum tunneling of the superconducting phase difference ϕ below the Josephson potential barrier connecting two energy minima at $\phi = 0, 2\pi$.

The situation becomes more interesting if the Cooper pair tunneling is mediated by a single transport channel with high transparency [18]. In this limit, the energy spectrum of the Josephson junction is characterized by a

narrowly avoided level crossing at $\phi = \pi$, and imaginary-time Landau-Zener (ITLZ) tunneling [18,19] acts to prevent quantum tunneling trajectories from reaching the energy minimum at 2π . The charge dispersion of the superconducting island then vanishes completely as the transparency approaches unity. While some weak suppression of Coulomb oscillations has been observed in weak links [20,21], the effect of ITLZ tunneling on charging effects has eluded experimental verification because of the stringent requirements for ballistic Josephson junctions. However, recent advances in nanofabrication and nanowire growth [22] have enabled the development of superconductor-semiconductor-superconductor junctions with a small number of highly transmitting modes [23,24]. Experiments in such devices have detected a single mode with nearly perfect transmission, attributed to resonant tunneling through an accidental quantum dot in the junction [25,26]. Charge-sensitive devices connected to reservoirs via quantum-dot-based junctions are thus ideal for the investigation of near-ballistic Josephson junction behavior.

In this Letter, we experimentally investigate the charge dispersion of a superconducting island connected to a reservoir via a semiconducting weak link hosting a quantum dot. The device constitutes an offset-charge-sensitive (OCS) nanowire transmon, also known as a gatemon [27–30]. By *in situ* tuning of the transparency of the weak link using an electrostatic gate, we observe its charge dispersion decrease by almost two decades in frequency at a rate far exceeding exponential suppression in E_J/E_c . The observed gate dependence of the charge dispersion is modeled by tunneling through a resonant level, incorporating the effect of ITLZ tunneling. This model agrees well with the measured suppression of charge dispersion, suggesting near-unity junction transparency. Finally, we

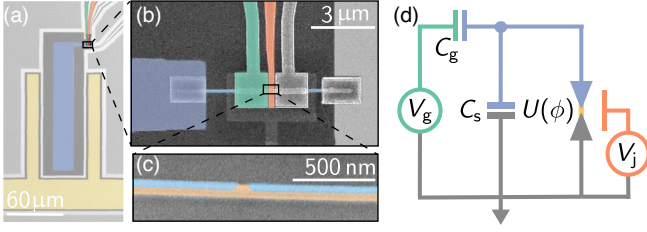


FIG. 1. (a) False-color optical microscope image of the qubit. It consists of an island (purple) capacitively coupled to the ground plane (gray) and a coplanar waveguide resonator (yellow). (b) Scanning electron micrograph (SEM) of the InAs-Al nanowire connecting the island (left) to the ground plane (right). Its weak link is tuned by the junction gate (red), while the island gate (green) tunes n_g on the island. Unused gates are left uncolored. (c) False-color SEM of the nanowire before deposition of the top gates, showing the InAs core (orange) and the aluminum shell (blue). (d) Effective circuit diagram of the qubit. The weak link with Josephson potential $U(\phi)$ is shunted by the island capacitance C_s , V_g tunes n_g , and V_j tunes the transparency of the junction.

observe improved qubit coherence times T_2^* and T_2^{echo} in regions of vanishing charge dispersion, which reflects the strong reduction in the charge sensitivity of the qubit.

The measured gatemon is shown in Fig. 1. The details of the device and experimental setup are provided in Ref. [31], so we highlight only the relevant features here. The device consists of a superconducting island coupled to ground via an Al/InAs/Al weak link [22,27,28]. The weak link [shown in Fig. 1(c)] is defined by etching away ~ 100 nm of the aluminum covering the InAs nanowire. A quantum dot is formed in the junction due to band bending or disorder [32,33]. The junction is shunted by the island capacitance C_s , which predominantly sets the charging energy $E_c \approx 750$ MHz. Electrostatic gates tune both the transparency of the junction and the dimensionless offset charge $n_g = C_g V_g / 2e$ on the island. The gatemon is capacitively coupled to a NbTiN $\lambda/2$ coplanar waveguide resonator [34] in order to excite and read out the system using standard dispersive readout techniques [35].

We measure the dependence of qubit's ground to first excited state transition frequency on the offset charge on the island [$f_{01}(n_g)$] using two-tone spectroscopy, as shown in Fig. 2(a). Each measurement results in two sinusoidal curves shifted by half a period, belonging to qubit transitions for even and odd island parity. Their simultaneous detection is due to quasiparticle poisoning on timescales faster than the measurements [36,37]. We define the qubit frequency f_{01} as the point of charge degeneracy between even and odd island parity and the charge dispersion δf_{01} as the maximal frequency difference between the two parity states, reflecting the maximal energy cost of charging the island with an additional electron.

Figure 2(a) also demonstrates the behavior of $\{f_{01}, \delta f_{01}\}$ at different V_j near full depletion of the junction. In the

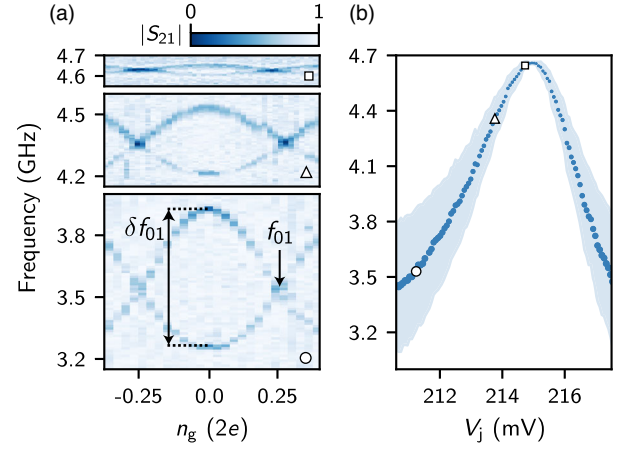


FIG. 2. Evolution of the qubit frequency and charge dispersion as a function of V_j . (a) Normalized two-tone spectroscopy measurements of the $0 \rightarrow 1$ transition versus the offset charge tuned by V_g , measured at three successive values of V_j : 211.2, 213.8, and 214.7 mV. (b) Extracted f_{01} (markers) and δf_{01} (shading and marker size) versus V_j . Open markers indicate the positions of (a).

lowest panel, we observe $f_{01} = 3.539$ GHz and $\delta f_{01} = 679$ MHz at $V_j = 211.2$ mV. As V_j is increased, in the middle and top panel of Fig. 2(a), f_{01} increases to 4.629 GHz, while δf_{01} decreases to 39 MHz. Figure 2(b) summarizes the dependence of f_{01} and δf_{01} as a function of V_j . We observe that the qubit frequency exhibits a peak, increasing by a factor of 1.35 before decreasing again. The rise in f_{01} is accompanied by a strong decrease in δf_{01} , suppressing by almost 2 orders of magnitude at the peak. This behavior is consistent with the presence of a quantum dot in the junction, which has been linked to peaks in the critical current that coincide with transparencies close to unity [25,26].

Because of finite stray capacitance, the transparency of the junction can also be tuned using the island gate. As shown in Fig. 3(a), we observe suppression of the charge dispersion by tuning the island gate voltage V_g with V_j fixed at a value where the charge dispersion is already close to the qubit linewidth $\gamma_{01} \approx 10$ MHz [38]. We note that δf_{01} can no longer be discerned below γ_{01} since the two parity transitions start to overlap.

We can probe the suppression of Coulomb oscillations to below the limit set by γ_{01} by measuring the charge dispersion of higher-order qubit transitions, which have a rapidly increasing charge dispersion δf_{0n} [16,18]. We repeat the measurement for increased driving powers in order to excite higher-order qubit transitions. As shown in Figs. 3(b) and 3(c), the $0 \rightarrow 2$ and $0 \rightarrow 3$ multiphoton transitions indeed exhibit larger charge dispersion than the $0 \rightarrow 1$ transition. Even these larger charge dispersions vanish down to the linewidth γ_{0n} , indicating a particularly strong suppression.

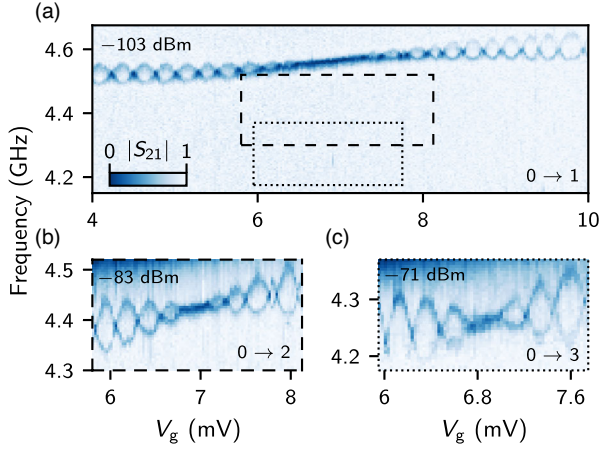


FIG. 3. Island gate dependence of the charge dispersion. (a) Normalized two-tone spectroscopy measurement of the $0 \rightarrow 1$ transition over a range of V_g encompassing many periods in offset charge. The charge dispersion suppresses down to the linewidth and subsequently recovers, while the qubit frequency increases over the entire gate range. (b), (c) Multiphoton transitions $0 \rightarrow 2$ and $0 \rightarrow 3$, excited with increased driving powers. The transitions follow the same trends as (a), exhibiting an increased charge dispersion that still suppresses down to the linewidth at its minimum. Powers listed are at the sample input.

Beyond the remarkable suppression of the charge dispersion, we note that δf_{01} does not depend monotonically on f_{01} . The charge dispersion of the $0 \rightarrow 1$ transition is suppressed down to the linewidth over several periods, while the qubit frequency slowly increases over the entire range of V_g . Such a dependence cannot occur for

superconducting tunnel junctions or a single-mode superconducting quantum point contact (SQPC) [39], where larger qubit frequencies always result in lower charge dispersions [16,18]. This behavior is the result of the quantum dot in the junction, in which case the charge dispersion need not be a monotonic function of the qubit frequency, as we explain below.

We develop a quantitative understanding of the device using a simplified model of a quantum dot between two superconducting leads, known as the resonant level model [40–43]. As shown in Fig. 4(a), we consider the presence of a single spin-degenerate level in the junction. The level has an energy ϵ_0 relative to the Fermi level and is coupled to two identical superconductors with superconducting gap Δ via the (spin-degenerate) tunnel rates Γ_l and Γ_r . Our simple model does not include the electron-electron interactions of the quantum dot. The potential of the junction $U(\phi)$ is determined by the energies of a single pair of spin-degenerate Andreev bound state (ABS) [shown in Fig. 4(b)]. Their energies have to be calculated numerically for general parameter values, but can be expressed analytically in certain limits [42,43]

$$E_{\pm}(\phi) = \pm \tilde{\Delta} \sqrt{1 - \tilde{D} \sin^2 \phi / 2}, \quad \tilde{D} = \frac{4\Gamma_l \Gamma_r}{\epsilon_0^2 + \Gamma^2},$$

$$\tilde{\Delta} = \begin{cases} \Delta, & \text{if } \Gamma \gg \Delta, \epsilon_0 \\ \Gamma & \text{if } \Gamma \ll \Delta \text{ and } \epsilon_0 = 0, \end{cases} \quad (1)$$

where $\Gamma = \Gamma_l + \Gamma_r$. Here the ABS take on the same functional form as for a SQPC [44], but with an effective

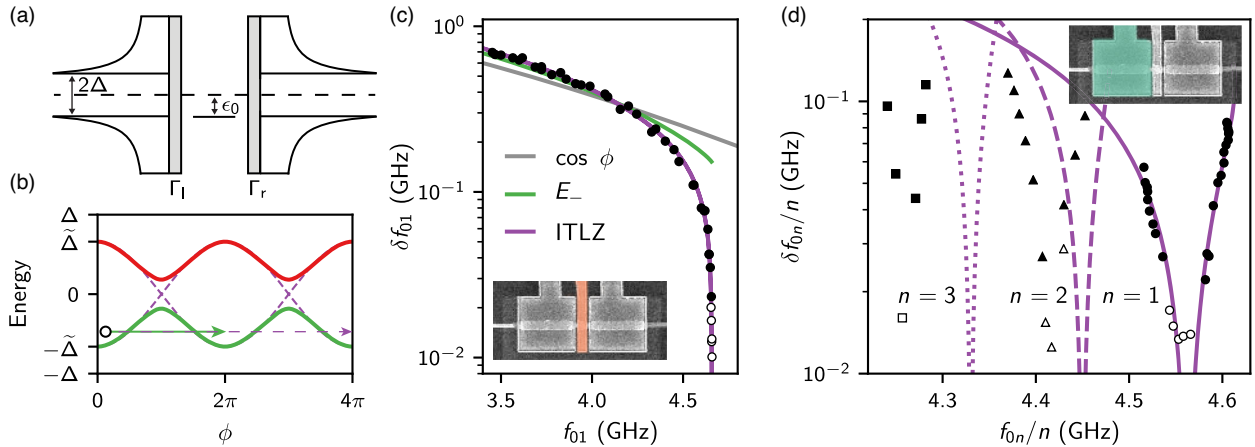


FIG. 4. Suppression of charge dispersion mediated by a resonant level. (a) Schematic depiction of a resonant level coupled to two identical superconducting leads. (b) Calculated energy-phase dependence of the ABS in the resonant level model for $\tilde{D} = 0.9$ (solid) and $\tilde{D} = 1$ (dashed) with $\Gamma = \Delta$. Arrows indicate the available quantum tunneling trajectories for the two cases. (c) Extracted qubit frequency versus charge dispersion measured in Fig. 2 by varying V_j . Solid lines show fits using three models of $U(\phi)$: a sinusoidal potential, the negative energy ABS branch of the resonant level model, and a potential considering ITLZ tunneling between both ABS branches. (d) Extracted qubit frequency and charge dispersion of the first three transmon transitions measured as a function of V_g shown in Fig. 3. The solid line shows a fit of the $0 \rightarrow 1$ transition with the ITLZ model, and the dashed and dotted lines show the resulting $0 \rightarrow 2$ and $0 \rightarrow 3$ transitions, respectively. Open markers denote an upper bound on the charge dispersion based on the linewidth when $\delta f_{0n} \leq \gamma_{0n}$ and are not included in the fits.

superconducting gap $\tilde{\Delta} < \Delta$. The form of the effective junction transparency \tilde{D} also explicitly reflects a Breit-Wigner-type resonant tunneling process, maximized for equal tunnel rates ($\delta\Gamma = |\Gamma_l - \Gamma_r| = 0$) and particle-hole symmetry ($\epsilon_0 = 0$).

We now discuss the expected behavior of charge dispersion within this model. Under the typical assumptions of low to moderate values of \tilde{D} and $\tilde{\Delta} \gg E_c, k_B T$, only the ground state of the junction is occupied so that charge transfer occurs through E_- . In this regime, charge dispersion is exponentially suppressed in $\tilde{\Delta} \tilde{D} / E_c$, comparable to the case of tunnel junctions and governed by tunneling of the phase under the potential barrier of E_- [16,17]. As $\tilde{D} \rightarrow 1$, however, the energy gap between the ABS vanishes. Because of ITLZ tunneling, the probability amplitude for the quantum tunneling trajectory to stay in the lower ABS branch vanishes linearly with the reflection amplitude $\sqrt{1 - \tilde{D}}$ [18,45]. As a consequence 2π tunneling processes are suppressed and so is the charge dispersion. When $\tilde{D} = 1$, the charge dispersion eventually saturates to a small value set by tunneling through a 4π -wide potential barrier given by $\tilde{\Delta} \cos \phi / 2$.

Based on the discussion above, we fit the measured dependence of $\{f_{0n}, \delta f_{0n}\}$ using three junction models: a sinusoidal potential, a potential considering only the E_- ABS branch of the resonant level model, and a potential including ITLZ tunneling. The numerical details of the procedure are described in the Supplemental Material [46]. In Fig. 4(c), we plot the measured data for the dependence of δf_{01} on f_{01} while V_j is changed. In order to fit the data, we assume that V_j tunes only ϵ_0 while $\Gamma_l = \Gamma_r$ are held constant. Furthermore, we fix $\Delta = 53$ GHz based on dc transport experiments on similar nanowires [33]. The model based on a sinusoidal potential, which describes a tunnel junction with many low-transmission channels, is completely inconsistent with our data. Including only the presence of E_- results in a fit that matches the initial decrease in δf_{01} , but is unable to capture the rapid suppression of the charge dispersion at the peak in qubit frequency. The model including ITLZ tunneling accurately describes the full range of data, requiring transparencies close to unity [46]. We find that $\Gamma = 23$ GHz, which gives an effective gap $\tilde{\Delta} = 16$ GHz at the point of maximal suppression. The data and fit clearly demonstrate reaching the diabatic regime of ITLZ tunneling.

We additionally use the model including ITLZ tunneling to fit the V_g dependence of $\{f_{0n}, \delta f_{0n}\}$ in Fig. 4(d). Based on the position of the island gate to the left of the junction, as well as screening by the junction gate, we assume that V_g tunes only Γ_l with all other parameters held constant. The resulting fit matches the characteristic shape of the data, showing strong suppression when $\delta\Gamma = 0$ and reproducing the nonmonotonic relationship between qubit frequency and dispersion. The measurements also show that the

anharmonicity $\alpha = f_{12} - f_{01}$ remains finite for all \tilde{D} , essential for operation as a qubit. While the fit is excellent for the $0 \rightarrow 1$ transition, it requires a significantly lower superconducting gap $\Delta = 18.6$ GHz. Additionally, the predicted qubit anharmonicities [indicated by the lines in Fig. 4(d)] are lower than the measured anharmonicities, while the shapes of the curves remain accurate. This systematic deviation indicates that the underlying junction potential might be shallower than captured by our model. We speculate that the discrepancies in Δ and the anharmonicities could be due to omitting the electron-electron interactions of the quantum dot, which has previously been found to suppress the critical current and alter the energy-phase dependence of the ABS [26,48–50].

Finally, we investigate the qubit's relaxation and coherence times in the presence and absence of resonant tunneling. Shown in Fig. 5, we compare two cases: strong ITLZ tunneling, with vanishing charge dispersion, and essentially adiabatic behavior with $\delta f_{01} \approx 200$ MHz. We leverage the nonmonotonic $\{f_{01}, \delta f_{01}\}$ dependence encoded by V_g to make this comparison at nominally equal transition frequency in the same device. We find that the suppression leads to a moderately enhanced T_1 . However, we do not expect charging effects to have a large effect on T_1 since the measurements are performed at $n_g = 0.5$, where relaxation processes should be mostly charge insensitive. We find, however, that both T_2^* and T_2^{echo} improve considerably for the case of vanishing charge dispersion, reflecting the drastic reduction in sensitivity to

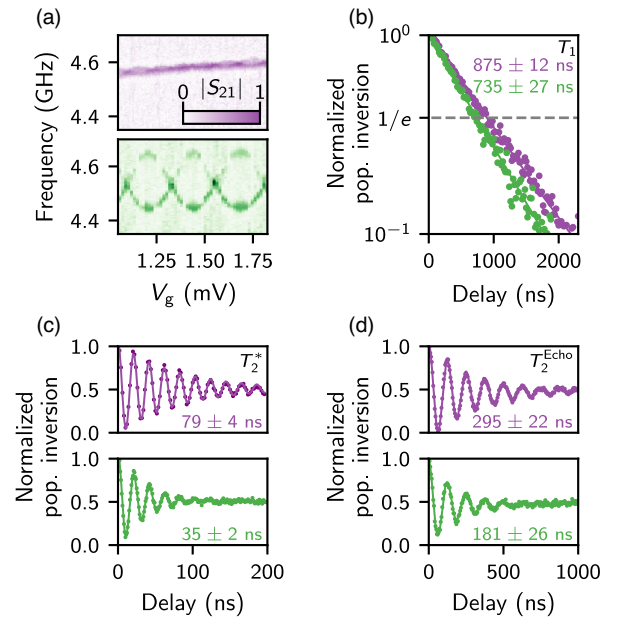


FIG. 5. Time-resolved qubit measurements for $\tilde{D} \rightarrow 1$ (purple) and $\tilde{D} \approx 0.8$ (green) in the junction measured at equal qubit frequency. (a) Two-tone spectroscopy measurements for the two cases. Also shown are measurements of (b) T_1 , (c) T_2^* , and (d) T_2^{Echo} .

charge noise. This is similar to the situation in conventional transmon qubits, where the exponential suppression of charge dispersion in E_J/E_C is also accompanied by a strong increase in coherence times [16]. However, in order to achieve the same level of δf_{01} suppression in a conventional transmon for the E_C of this device, one would require $E_J/E_C \geq 30$, whereas we are operating at an effective $E_J/E_C \approx 5$. Even in the limit of full suppression, however, both relaxation and coherence times are short compared to results achieved in other gatemons [51]. We attribute these lower coherence times to ineffective radiation shielding and the quality of dielectrics used, which can be improved in future devices.

In summary, we measure the suppression of charge dispersion in an OCS gatemon with a highly transparent junction. We develop a model of tunneling through a resonant level in the junction that agrees with the dependence of the charge dispersion on both gates and indicates that, through tuning the parameters of our resonant level properly, we reach near-unity transparencies in our device. Furthermore, the observed rate of suppression of the charge dispersion obeys the scaling law dictated by ITLZ tunneling between ABS. Finally, we demonstrate that the suppression improves the qubit's coherence, reflecting the strong decrease in charge sensitivity.

The vanishing of charging effects investigated here has implications for the design of hybrid circuits incorporating ballistic Josephson junctions [52–57]. In particular, this vanishing may have positive implications for future gatemons [27–30,51]. The guaranteed vanishing of charge sensitivity for $\tilde{D} \rightarrow 1$ while the anharmonicity remains finite places much less stringent requirements on E_C compared to other transmon implementations, allowing for faster qubit manipulation and strongly reducing the qubit's physical footprint. The natural magnetic field compatibility of superconductor-quantum dot-superconductor transmons also sets the stage for detecting and manipulating Majorana zero modes [19,58,59]. Finally, independent research reports similar results on the charge dispersion of a full-shell nanowire gatemon with a dc transport lead [60].

We acknowledge fruitful discussions with A. Antipov, A. Kringhøj, J. Kroll, T. W. Larsen, R. Lutchyn, K. Petersson, W. Pfaff, D. Pikulin, and A. Proutski. We further thank Jasper van Veen for placing the nanowire and Will Oliver for providing us with a traveling wave parametric amplifier. This work is part of the research project Scalable circuits of Majorana qubits with topological protection (i39, SCMQ) with Project No. 14SCMQ02, which is (partly) financed by the Dutch Research Council (NWO). It has further been supported by the Microsoft Quantum initiative.

* a.bargerbos@tudelft.nl

- [1] K. K. Likharev, Single-electron devices and their applications, *Proc. IEEE* **87**, 606 (1999).
- [2] S. Komiyama, O. Astafiev, V. Antonov, T. Kutsuwa, and H. Hirai, A single-photon detector in the far-infrared range, *Nature (London)* **403**, 405 (2000).
- [3] W. Lu, Z. Ji, L. Pfeiffer, K. W. West, and A. J. Rimberg, Real-time detection of electron tunnelling in a quantum dot, *Nature (London)* **423**, 422 (2003).
- [4] M. Meschke, J. Engert, D. Heyer, and J. P. Pekola, Comparison of Coulomb blockade thermometers with the international temperature scale PLTS-2000, *Int. J. Thermophys.* **32**, 1378 (2011).
- [5] J. P. Pekola, O. P. Saira, V. F. Maisi, A. Kemppinen, M. Möttönen, Y. A. Pashkin, and D. V. Averin, Single-electron current sources: Toward a refined definition of the ampere, *Rev. Mod. Phys.* **85**, 1421 (2013).
- [6] K. Flensberg, Capacitance and conductance of mesoscopic systems connected by quantum point contacts, *Phys. Rev. B* **48**, 11156 (1993).
- [7] K. A. Matveev, Coulomb blockade at almost perfect transmission, *Phys. Rev. B* **51**, 1743 (1995).
- [8] I. L. Aleiner and L. I. Glazman, Mesoscopic charge quantization, *Phys. Rev. B* **57**, 9608 (1998).
- [9] Y. V. Nazarov, Coulomb Blockade without Tunnel Junctions, *Phys. Rev. Lett.* **82**, 1245 (1999).
- [10] L. P. Kouwenhoven, N. C. van der Vaart, A. T. Johnson, W. Kool, C. J. Harmans, J. G. Williamson, A. A. Staring, and C. T. Foxon, Single electron charging effects in semiconductor quantum dots, *Z. Phys. B* **85**, 367 (1991).
- [11] L. W. Molenkamp, K. Flensberg, and M. Kemerink, Scaling of the Coulomb Energy Due to Quantum Fluctuations in the Charge on a Quantum Dot, *Phys. Rev. Lett.* **75**, 4282 (1995).
- [12] P. Joyez, V. Bouchiat, D. Esteve, C. Urbina, and M. H. Devoret, Strong Tunneling in the Single-Electron Transistor, *Phys. Rev. Lett.* **79**, 1349 (1997).
- [13] D. Chouvaev, L. S. Kuzmin, D. S. Golubev, and A. D. Zaikin, Strong tunneling and coulomb blockade in a single-electron transistor, *Phys. Rev. B* **59**, 10599 (1999).
- [14] S. Jezouin, Z. Iftikhar, A. Anthore, F. D. Parmentier, U. Gennser, A. Cavanna, A. Ouerghi, I. P. Levkivskiy, E. Idrisov, E. V. Sukhorukov, L. I. Glazman, and F. Pierre, Controlling charge quantization with quantum fluctuations, *Nature (London)* **536**, 58 (2016).
- [15] V. Bouchiat, D. Vion, P. Joyez, D. Esteve, and M. H. Devoret, Quantum Coherence with a Single Cooper Pair, *Phys. Scr.* **T76**, 165 (1998).
- [16] J. Koch, T. M. Yu, J. Gambetta, A. A. Houck, D. I. Schuster, J. Majer, A. Blais, M. H. Devoret, S. M. Girvin, and R. J. Schoelkopf, Charge-insensitive qubit design derived from the Cooper pair box, *Phys. Rev. A* **76**, 042319 (2007).
- [17] D. V. Averin, A. B. Zorin, and K. K. Likharev, Bloch oscillations in small Josephson junctions, *Zh. Eksp. Teor. Fiz.* (1985), <http://jetp.ac.ru/cgi-bin/e/index/e/61/2/p407?a=list>.
- [18] D. V. Averin, Coulomb Blockade in Superconducting Quantum Point Contacts, *Phys. Rev. Lett.* **82**, 3685 (1999).
- [19] D. Pikulin, K. Flensberg, L. I. Glazman, M. Houzet, and R. M. Lutchyn, Coulomb Blockade of a Nearly Open Majorana Island, *Phys. Rev. Lett.* **122**, 016801 (2019).
- [20] T. Lorenz, S. Sprenger, and E. Scheer, Coulomb Blockade and Multiple Andreev Reflection in a Superconducting

- Single-Electron Transistor, *J. Low Temp. Phys.* **191**, 301 (2018).
- [21] A. Proutski, D. Laroche, B. van 't Hooft, P. Krogstrup, J. Nygård, L. P. Kouwenhoven, and A. Geresdi, Broadband microwave spectroscopy of semiconductor nanowire-based Cooper-pair transistors, *Phys. Rev. B* **99**, 220504(R) (2019).
- [22] P. Krogstrup, N. L. Ziino, W. Chang, S. M. Albrecht, M. H. Madsen, E. Johnson, J. Nygård, C. M. Marcus, and T. S. Jespersen, Epitaxy of semiconductor-superconductor nanowires, *Nat. Mater.* **14**, 400 (2015).
- [23] D. J. Van Woerkom, A. Proutski, B. Van Heck, D. Bouman, J. I. Väyrynen, L. I. Glazman, P. Krogstrup, J. Nygård, L. P. Kouwenhoven, and A. Geresdi, Microwave spectroscopy of spinful Andreev bound states in ballistic semiconductor Josephson junctions, *Nat. Phys.* **13**, 876 (2017).
- [24] M. F. Goffman, C. Urbina, H. Pothier, J. Nygard, C. M. Marcus, and P. Krogstrup, Conduction channels of an InAs-Al nanowire Josephson weak link, *New J. Phys.* **19** (2017).
- [25] E. M. Spanton, M. Deng, S. Vaitiekenas, P. Krogstrup, J. Nygård, C. M. Marcus, and K. A. Moler, Current-phase relations of few-mode InAs nanowire Josephson junctions, *Nat. Phys.* **13**, 1177 (2017).
- [26] S. Hart, Z. Cui, G. Ménard, M. Deng, A. E. Antipov, R. M. Lutchyn, P. Krogstrup, C. M. Marcus, and K. A. Moler, Current-phase relations of InAs nanowire Josephson junctions: From interacting to multimode regimes, *Phys. Rev. B* **100**, 064523 (2019).
- [27] G. de Lange, B. van Heck, A. Bruno, D. J. van Woerkom, A. Geresdi, S. R. Plissard, E. P. A. M. Bakkers, A. R. Akhmerov, and L. DiCarlo, Realization of Microwave Quantum Circuits Using Hybrid Superconducting-Semiconducting Nanowire Josephson Elements, *Phys. Rev. Lett.* **115**, 127002 (2015).
- [28] T. W. Larsen, K. D. Petersson, F. Kuemmeth, T. S. Jespersen, P. Krogstrup, J. Nygård, and C. M. Marcus, Semiconductor-Nanowire-Based Superconducting Qubit, *Phys. Rev. Lett.* **115**, 127001 (2015).
- [29] A. Kringhøj, L. Casparis, M. Hell, T. W. Larsen, F. Kuemmeth, M. Leijnse, K. Flensberg, P. Krogstrup, J. Nygård, K. D. Petersson, and C. M. Marcus, Anharmonicity of a superconducting qubit with a few-mode Josephson junction, *Phys. Rev. B* **97**, 060508 (2018).
- [30] K. Serniak, S. Diamond, M. Hays, V. Fatemi, S. Shankar, L. Frunzio, R. J. Schoelkopf, and M. H. Devoret, Direct Dispersive Monitoring of Charge Parity in Offset-Charge-Sensitive Transmons, *Phys. Rev. Applied* **12**, 014052 (2019).
- [31] W. Uilhoorn, Parity lifetime of a proximitized semiconductor nanowire qubit in magnetic field (to be published).
- [32] W. Chang, S. M. Albrecht, T. S. Jespersen, F. Kuemmeth, P. Krogstrup, J. Nygård, and C. M. Marcus, Hard gap in epitaxial semiconductor-superconductor nanowires, *Nat. Nanotechnol.* **10**, 232 (2015).
- [33] M. T. Deng, S. Vaitiekenas, E. B. Hansen, J. Danon, M. Leijnse, K. Flensberg, J. Nygård, P. Krogstrup, and C. M. Marcus, Majorana bound state in a coupled quantum-dot hybrid-nanowire system, *Science* **354**, 1557 (2016).
- [34] J. G. Kroll, F. Borsoi, K. L. van der Enden, W. Uilhoorn, D. de Jong, M. Quintero-Pérez, D. J. van Woerkom, A. Bruno, S. R. Plissard, D. Car, E. P. A. M. Bakkers, M. C. Cassidy, and L. P. Kouwenhoven, Magnetic-Field-Resilient Superconducting Coplanar-Waveguide Resonators for Hybrid Circuit Quantum Electrodynamics Experiments, *Phys. Rev. Applied* **11**, 064053 (2019).
- [35] R. Bianchetti, S. Filipp, M. Baur, J. M. Fink, M. Göppl, P. J. Leek, L. Steffen, A. Blais, and A. Wallraff, Dynamics of dispersive single-qubit readout in circuit quantum electrodynamics, *Phys. Rev. A* **80**, 043840 (2009).
- [36] J. A. Schreier, A. A. Houck, J. Koch, D. I. Schuster, B. R. Johnson, J. M. Chow, J. M. Gambetta, J. Majer, L. Frunzio, M. H. Devoret, S. M. Girvin, and R. J. Schoelkopf, Suppressing charge noise decoherence in superconducting charge qubits, *Phys. Rev. B* **77**, 180502 (2008).
- [37] Measurements are integrated for 50 ms, while quasiparticle poisoning takes place on a timescale of $\sim 100 \mu\text{s}$ [31].
- [38] These measurements are performed in a different cooldown of the same device.
- [39] C. W. J. Beenakker and H. van Houten, The superconducting quantum point contact, *Nanostructures and Mesoscopic systems*, 481, (1992)
- [40] L. Glazman and K. Matveev, Resonant Josephson current through Kondo impurities in a tunnel barrier, *JETP Lett.* **49**, 659 (1989), http://www.jetpletters.ac.ru/ps/1121/article_16988.shtml.
- [41] C. W. J. Beenakker and H. van Houten, Resonant josephson current through a quantum dot, in *Single-Electron Tunneling and Mesoscopic Devices*, edited by H. Koch and H. Lübbig, Springer Series in Electronics and Photonics Vol. 31 (Springer, Berlin, Heidelberg, 1992).
- [42] I. A. Devyatov and M. Y. Kupriyanov, Resonant Josephson tunneling through S-I-S junctions of arbitrary size, *J. Exp. Theor. Phys.* **85**, 189 (1997).
- [43] A. A. Golubov, M. Y. Kupriyanov, and E. Il'ichev, The current-phase relation in Josephson junctions, *Rev. Mod. Phys.* **76**, 411 (2004).
- [44] C. W. J. Beenakker, Universal Limit of Critical-Current Fluctuations in Mesoscopic Josephson Junctions, *Phys. Rev. Lett.* **67**, 3836 (1991).
- [45] D. A. Ivanov and M. V. Feigel'man, Coulomb effects in a ballistic one-channel S-S device, *Phys. Usp.* **41**, 197 (1998).
- [46] See Supplemental Material at <http://link.aps.org/supplemental/10.1103/PhysRevLett.124.246802> for details of the data extraction, modeling of the ITLZ tunneling, the effective resonant level model, the fitting procedure, and the estimation of the junction transparencies, which includes Ref. [47].
- [47] D. A. Ivanov and M. V. Feigel'man, Two-level Hamiltonian of a superconducting quantum point contact, *Phys. Rev. B* **59**, 8444 (1999).
- [48] E. Vecino, A. Martín-Rodero, and L. Yeyati, Josephson current through a correlated quantum level: Andreev states and π junction behavior, *Phys. Rev. B* **68**, 035105 (2003).
- [49] J. S. Lim and M.-S. Choi, Andreev bound states in the Kondo quantum dots coupled to superconducting leads, *J. Phys. Condens. Matter* **20**, 415225 (2008).
- [50] A. Martín-Rodero and A. Levy Yeyati, Josephson and Andreev transport through quantum dots, *Adv. Phys.* **60**, 899 (2011).

- [51] F. Luthi, T. Stavenga, O. W. Enzing, A. Bruno, C. Dickel, N. K. Langford, M. A. Rol, T. S. Jespersen, J. Nygård, P. Krogstrup, and L. DiCarlo, Evolution of Nanowire Transmon Qubits and Their Coherence in a Magnetic Field, *Phys. Rev. Lett.* **120**, 100502 (2018).
- [52] M. Chauvin, P. Vom Stein, D. Esteve, C. Urbina, J. C. Cuevas, and A. L. Yeyati, Crossover from Josephson to Multiple Andreev Reflection Currents in Atomic Contacts, *Phys. Rev. Lett.* **99**, 067008 (2007).
- [53] L. Bretheau, Ç. Ö. Girit, H. Pothier, D. Esteve, and C. Urbina, Exciting Andreev pairs in a superconducting atomic contact, *Nature (London)* **499**, 312 (2013).
- [54] D. Pekker, C. Y. Hou, V. E. Manucharyan, and E. Demler, Proposal for Coherent Coupling of Majorana Zero Modes and Superconducting Qubits Using the 4π Josephson Effect, *Phys. Rev. Lett.* **111**, 107007 (2013).
- [55] M. Hays, G. de Lange, K. Serniak, D. J. van Woerkom, D. Bouman, P. Krogstrup, J. Nygård, A. Geresdi, and M. H. Devoret, Direct Microwave Measurement of Andreev-Bound-State Dynamics in a Semiconductor-Nanowire Josephson Junction, *Phys. Rev. Lett.* **121**, 047001 (2018).
- [56] L. Tosi, C. Metzger, M. F. Goffman, C. Urbina, H. Pothier, S. Park, A. L. Yeyati, J. Nygård, and P. Krogstrup, Spin-Orbit Splitting of Andreev States Revealed by Microwave Spectroscopy, *Phys. Rev. X* **9**, 011010 (2019).
- [57] J. I. Wang, D. Rodan-Legrain, L. Bretheau, D. L. Campbell, B. Kannan, D. Kim, M. Kjaergaard, P. Krantz, G. O. Samach, F. Yan, J. L. Yoder, K. Watanabe, T. Taniguchi, T. P. Orlando, S. Gustavsson, P. Jarillo-Herrero, and W. D. Oliver, Coherent control of a hybrid superconducting circuit made with graphene-based van der Waals heterostructures, *Nat. Nanotechnol.* **14**, 120 (2018).
- [58] F. Hassler, A. R. Akhmerov, and C. W. Beenakker, The top-transmon: A hybrid superconducting qubit for parity-protected quantum computation, *New J. Phys.* **13**, 095004 (2011).
- [59] E. Ginossar and E. Grosfeld, Microwave transitions as a signature of coherent parity mixing effects in the Majorana-transmon qubit, *Nat. Commun.* **5**, <https://doi.org/10.1038/ncomms5772> (2014).
- [60] A. Kringhøj, B. van Heck, T. W. Larsen, O. Erlandsson, D. Sabonis, P. Krogstrup, L. Casparis, K. D. Petersson, and C. M. Marcus, following Letter, Suppressed Charge Dispersion via Resonant Tunneling in a Single-Channel Transmon, *Phys. Rev. Lett.* **124**, 246803 (2020).